# Momentum transfer of a Boltzmann-lattice fluid with boundaries

M'hamed Bouzidi, Mouaouia Firdaouss, and Pierre Lallemand

Citation: Phys. Fluids **13**, 3452 (2001); doi: 10.1063/1.1399290
View online: http://dx.doi.org/10.1063/1.1399290
View Table of Contents: http://pof.aip.org/resource/1/PHFLE6/v13/i11
Published by the AIP Publishing LLC.

# Momentum transfer of a Boltzmann-lattice fluid with boundaries

M'hamed Bouzidi[a)]
*Laboratoire C.N.R.S.-A.S.C.I., Bâtiment 506, Université Paris-Sud (Paris XI Orsay), 91405 Orsay Cedex, France*

Mouaouia Firdaouss[b)]
*Laboratoire C.N.R.S.-L.I.M.S.I., Bâtiment 508, Université Paris-Sud (Paris XI Orsay), 91405 Orsay Cedex, France*

Pierre Lallemand[c)]
*Laboratoire C.N.R.S.-A.S.C.I., Bâtiment 506, Université Paris-Sud (Paris XI Orsay), 91405 Orsay Cedex, France*

(Received 5 July 2000; accepted 5 June 2001)

We study the velocity boundary condition for curved boundaries in the lattice Boltzmann equation (LBE). We propose a LBE boundary condition for moving boundaries by combination of the ''bounce-back'' scheme and spatial interpolations of first or second order. The proposed boundary condition is a simple, robust, efficient, and accurate scheme. Second-order accuracy of the boundary condition is demonstrated for two cases: (1) time-dependent two-dimensional circular Couette flow and (2) two-dimensional steady flow past a periodic array of circular cylinders (flow through the porous media of cylinders). For the former case, the lattice Boltzmann solution is compared with the analytic solution of the Navier–Stokes equation. For the latter case, the lattice Boltzmann solution is compared with a finite-element solution of the Navier–Stokes equation. The lattice Boltzmann solutions for both flows agree very well with the solutions of the Navier–Stokes equations. We also analyze the torque due to the momentum transfer between the fluid and the boundary for two initial conditions: (a) impulsively started cylinder and the fluid at rest, and (b) uniformly rotating fluid and the cylinder at rest.  [DOI: 10.1063/1.1399290]

## I. INTRODUCTION

The lattice gas automaton, a very simplified description of the dynamics of a real fluid using an ensemble of fictitious particles that move synchronously on a highly symmetric lattice from one node to one of the neighboring nodes,[1,2] together with its analysis in terms of the lattice Boltzmann equation (LBE) provides an efficient alternative[3–8] for direct numerical simulations of the Navier–Stokes equations at moderate Reynolds numbers.[9] Numerous papers have been devoted to the correspondence between the large scale properties of the solutions of the lattice Boltzmann equation and those of the continuous Navier–Stokes equation using either the Chapman–Enskog analysis[10] or an analysis of the time evolution of moments of distribution functions.[11]

One important and outstanding problem in the lattice Boltzmann method is that of boundary conditions. To include boundaries in the LBE simulations, several schemes have been proposed in the past to satisfy locally the standard ''no-slip'' or ''free-slip'' conditions of macroscopic flows.[12–18] The earliest ones in terms of ''bounce-back'' (or ''specular reflection'')[2] were shown to be satisfactory for boundaries parallel to one of the discrete velocities of the model provided one is careful enough about their exact location. For general boundaries it was found necessary to consider some kind of average over a region including several lattice nodes which led to mean boundary conditions.[19–21] This is physically sound as the relaxational nature of the dynamics acts as a low-pass spatial frequency filter which erases the details of the representation of a smooth boundary by a series of linear steps drawn on the underlying lattice.

To obtain macroscopic information about the flows simulated by using the LBE method, one relies on the fact that the LBE technique provides direct information about the single particle distribution function in phase space, with a very small set of discrete particle velocities. Based upon the distribution function, macroscopic information on the flow, such as flow velocity and local pressure distributions, can be easily determined. From this information one can in principle compute quantities such as drag or lift coefficients.

When a boundary of some type is present, the fluid–boundary interaction determines the momentum transfer of all the particles that encounter the boundary, and in turn affects the distribution function at the boundary. In the LBE method, the fluid–boundary interaction is prescribed to obtain desirable macroscopic boundary conditions for the corresponding hydrodynamic situations described by the Navier–Stokes equations. The key in analyzing the LBE boundary conditions is to realize the locations of the effective boundary for certain fluid–boundary interactions where the desirable macroscopic boundary conditions are satisfied to a certain extent.[19–21]

In this paper a simple way to deal with boundaries of

a)Electronic mail: bouizidi@asci.fr
b)Electronic mail: firdaous@limsi.fr
c)Electronic mail: lalleman@asci.fr

 

arbitrary geometry in the LBE method is proposed, combining the intuitive notion of ''bounce-back'' and interpolations. It is computationally efficient and compatible with the philosophy of LBE techniques in terms of accuracy and ease of implementation through the use of a lattice of high symmetry. This differs from standard CFD techniques which use nonuniform meshes that are chosen to match solid boundaries and the application of these ideas to LBE.[9,22]

This paper is organized as follows. Section II briefly reviews the lattice Boltzmann equation and its extension—the generalized lattice Boltzmann equation.[11] Section III describes the proposed boundary condition for arbitrary boundary geometry. In Sec. IV we compare the results of LBE simulations for Poiseuille flow in a two-dimensional channel using our proposed boundary conditions. Section V presents the numerical results of the two-dimensional circular Couette flow by using the LBE method with the proposed boundary condition, and the numerical results are compared with the analytic solution of the Navier–Stokes equations. Section VI considers the momentum transfer between fluid and boundary. The time-dependent torque exerted on the boundary from the fluid in the two-dimensional circular Couette flow of Sec. V is considered in two settings: (1) the circular boundary impulsively starts, while the fluid is at rest; and (2) the fluid is initially in uniform circular motion, and the boundary is maintained at rest. The numerical results for the torque are compared with the analytic solution of the Navier–Stokes equation. Section VII presents the LBE simulation of the flow past a periodic array of cylinders. The permeability coefficient is computed as a function of the volume fraction. The LBE results are compared to those of a finite element CFD computation. Section VIII concludes the paper.

## II. DEFINITION OF LBE SIMULATIONS

For the sake of simplicity without losing any generality, we shall consider a simple nine-velocity model on a square lattice, in which particles move with one of nine possible velocities $\mathbf{c}_i, i \in \{0,1,...,8\}$

$$\mathbf{c}_i = \begin{cases} (0,0), & i=0 \\ (\cos[(i-1)\pi/2], \sin[(i-1)\pi/2]), & i=1-4 \\ (\cos[(2i-9)\pi/4], \sin[(2i-9)\pi/4])\sqrt{2}, & i=5-8, \end{cases} \tag{1}$$

where we use nondimensionalized quantities after taking 1 for the size of the unit cell of the lattice and 1 for the duration of the time step.

The state of the fluid is completely known once we have determined at each time step and each *fluid* lattice node [we distinguish *fluid* and *solid* lattice nodes, the latter being located inside (outside) boundaries, for the case of an external (internal) flow] nine quantities $f_i(\mathbf{r},t)$ that can be interpreted as populations of the nine velocities $\mathbf{c}_i$.

We denote $\mathbf{F}(\mathbf{r},t)$ the following vector in a nine-dimensional space:

$$\mathbf{F} = (f_0, f_1, f_2, f_3, f_4, f_5, f_6, f_7, f_8).$$

The dynamics of $\mathbf{F}$ includes two steps: collision and advection to the relevant neighbors. We note the state after collision with a superscript $c$ and the state after collision and advection with $t+1$ for the value of the time. It is represented by the lattice Boltzmann equation

$$\mathbf{F}(\mathbf{r}_l + \mathbf{c}_i, t+1) = \mathbf{F}(\mathbf{r}_l, t) + \mathcal{C}\mathbf{F}(\mathbf{r}_l, t), \tag{2}$$

where $\mathbf{r}_l$ is the location of a lattice node. The collision operator $\mathcal{C}$ corresponds to the redistribution of the $f_i$ due to collisions to give $f_i^c(\cdot,t)$. Propagation (or advection) is then applied to give the final values $f_i(\cdot + \mathbf{c}_i, t+1)$.

In the bulk of the fluid, collisions can be implemented using the simple BGK model,[7] which is the result in a compact form of the following operations. At each node one computes a set of nine moments of the incoming distribution $\mathbf{F}$ through the linear transformation (see Refs. 11 and 23)

$$\mathbf{M} = \mathcal{M}\mathbf{F}. \tag{3}$$

The matrix $\mathcal{M}$ is given in Ref. 23 for the present nine-velocity model. It can be obtained fairly simply for other cases. Collisions modify the moments in the following way: some of them are conserved (density and momentum but not energy in usual cases). Other moments are computed through a simple linear relaxation equation toward equilibrium values that depend on the conserved quantities. The new state $\mathbf{F}^c$ is then computed from the new moments,

$$\mathbf{F}^c = \mathcal{M}^{-1}\mathbf{M}^c. \tag{4}$$

When a single relaxation time is used as in the BGK model, simplified formulas can be derived so that moments do not appear in Ref. 7. We prefer to keep the possibility of using different relaxation rates as proposed in the multiple relaxation times model.[11] The slight increase in computational cost is worthwhile at least for two reasons:

(1) The stability can be significantly improved.[23]
(2) The bulk viscosity can be chosen much larger than the shear viscosity, so that acoustic modes can be attenuated very quickly, which may be very useful in some situations.

Advection to neighbors is straightforward except at nodes close to a boundary as ''solid'' nodes inside the boundary cannot be reached. It is the purpose of this paper to describe a simple and efficient way out of this problem.

## III. BOUNDARY CONDITIONS

### A. Fixed boundaries

To deal with the advection step in the presence of boundaries we use an intuitive approach based on the one-dimensional situation depicted in Fig. 1. Fluid nodes are on the left with $A$ being the last one near the wall. $B$ is the first solid node to the right of the wall. The location of the wall is given by $q = |AC|/|AB|$. A particle leaving $A$ and reflecting on the wall (''bounce-back'' situation) will not reach a fluid node after moving over a total distance of 1 (case of velocity 1) except if $q$ is equal to 0, 1/2, or 1. This means that after the collision step the population of particles at $A$ with velocity $-1$ (indicated by the vector with label $L$) is not known. We propose the following scheme.

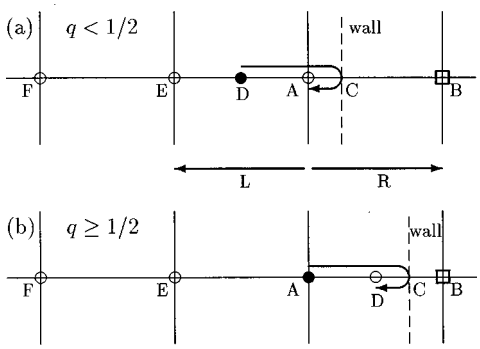


FIG. 1. Details of the collision process for velocities of opposite direction.

(1) For $q<1/2$, we construct from the information we have in the fluid the population of fictitious particles at location $D$ that will travel to $A$ after bouncing back on the wall at $C$.
(2) For $q\geqslant 1/2$, the information on the particle leaving $A$ and arriving in $D$ together with the new (postadvection) situation at fluid nodes $E$ (and $F$) will be used to compute the unknown quantities at $A$.

In both cases we use linear or quadratic interpolation formulas involving values at two or three nodes.

For real computations in two (or three) dimensions, we proceed in the following way. We first look for all links of the lattice that cross the solid boundary. Suppose $\mathbf{r}_l$ is a fluid node such that $\mathbf{r}_l+\mathbf{c}_i$ is a solid node. Call $\mathbf{c}_{i'}$ the reversed velocity of $\mathbf{c}_i(\mathbf{c}_{i'}=-\mathbf{c}_i)$. Using linear interpolation (interpolation 1) we set

$$f_{i'}(\mathbf{r}_l,t+1)=2qf_i^c(\mathbf{r}_l,t)+(1-2q)f_i^c(\mathbf{r}_l-\mathbf{c}_i,t), \quad q<\tfrac{1}{2}, \tag{5a}$$

$$f_{i'}(\mathbf{r}_l,t+1)=\frac{1}{2q}f_i^c(\mathbf{r}_l,t)+\frac{(2q-1)}{2q}f_{i'}^c(\mathbf{r}_i,t), \quad q\geqslant\frac{1}{2}. \tag{5b}$$

On the right hand-side of Eqs. (5a) and 5(b), the $f^c$ are taken after collision and before propagation. The $f(\cdot,t+1)$ on the left-hand side will be used at values after collision and after propagation, that is after a complete LBE time step. This means that the dynamics at nodes close to a boundary and at bulk nodes differ only in the propagation step.

The reason for using two different expressions depending on the value of $q$ is the following. When analyzed[23] in terms of modes varying in space as $\exp(i\mathbf{k}\cdot\mathbf{r})$ the LBE models usually present marginally stable modes with eigenvalue $-1$ [time evolution as $(-1)^t$] for $k=\pi$. Modification of the evolution equations involving products of $f_i$ by a negative factor may lead to instabilities that cannot be tolerated.

One can also use quadratic interpolation (interpolation 2) to obtain

$$f_{i'}(\mathbf{r}_l,t+1)=q(2q+1)f_i^c(\mathbf{r}_l,t)+(1+2q)\times(1-2q)f_i^c(\mathbf{r}_l-\mathbf{c}_i,t)-q(1-2q)\times f_i^c(\mathbf{r}_l-2\mathbf{c}_i,t), \quad q<\tfrac{1}{2}, \tag{6a}$$

$$f_{i'}(\mathbf{r}_l,t+1)=\frac{1}{q(2q+1)}f_i^c(\mathbf{r}_l,t)+\frac{(2q-1)}{q}f_{i'}^c(\mathbf{r}_l,t)+\frac{(1-2q)}{(1+2q)}f_{i'}^c(\mathbf{r}_l-\mathbf{c}_i,t), \quad q\geqslant\frac{1}{2}. \tag{6b}$$

Note that Eq. (6a) is an upwind interpolation, while Eq. (6b) is a downwind interpolation.

For completeness, we recall the usual ''bounce-back'' scheme without interpolation (interpolation 0),

$$f_{i'}(\mathbf{r}_l,t+1)=f_i^c(\mathbf{r}_l,t) \tag{7}$$

whatever the value of $q$.

A few comments on Eqs. (5), (6a), and (6b) are in order. First of all, in contrast to some other schemes which use extrapolations,[17,24] the proposed scheme uses only interpolations, therefore it is superior in terms of stability. Second, the change in $q$ is continuous in Eqs. (5), (6a), and (6b), and when $q=1/2$, the interpolation formulas reduce to the ''bounce-back'' scheme. It is much less complicated than that of Ref. 21 as we consider that the interaction of the fluid with the boundary couples only populations $f_i, f_{i'}$ with opposite velocities.

### B. Moving boundary

Equations (5), (6a), and (6b) are valid for boundaries at rest. For boundary with nonzero velocity we use a simple argument to deal with first-order contributions in wall motion. Let us refer again to Fig. 1. Assume that the macroscopic velocity $\mathbf{V}$ of the fluid to be simulated by the LBE scheme varies linearly along EB, taking value $\mathbf{V}_0$ at C (on the wall),

$$\mathbf{V}=\mathbf{V}_0+(x-q)\frac{\partial\mathbf{V}}{\partial x} \tag{8}$$

with $A$ as origin for the coordinate $x$. To first order in $V$ the equilibrium values of the $f_i$ are given by

$$f_i=f_i^0+\alpha_i\mathbf{c}_i\cdot\mathbf{V}, \tag{9}$$

where the coefficients $\alpha_i$ depend on the set of velocities of the LBE model. For the simple nine-velocity model,

$$\alpha_i=\{0,\tfrac{1}{3},\tfrac{1}{3},\tfrac{1}{3},\tfrac{1}{3},\tfrac{1}{12},\tfrac{1}{12},\tfrac{1}{12},\tfrac{1}{12}\}, \tag{10}$$

$$f_i^0=\{\tfrac{4}{9},\tfrac{1}{9},\tfrac{1}{9},\tfrac{1}{9},\tfrac{1}{9},\tfrac{1}{36},\tfrac{1}{36},\tfrac{1}{36},\tfrac{1}{36}\}. \tag{11}$$

Equating the corresponding value of $f_{i'}$ with that given by Eq. (5) leads to an additional term due to the motion of the boundary to be added to the right-hand side of Eqs. (5a) and (5b),

$$\delta f_{i'}^{(1)}=2\alpha_i\mathbf{c}_i\mathbf{V}_0, \quad q<\tfrac{1}{2}, \tag{12}$$

$$\delta f_{i'}^{(1)}=\frac{1}{q}\alpha_i\mathbf{c}_i\cdot\mathbf{V}_0, \quad q\geqslant\tfrac{1}{2}. \tag{13}$$

When the quadratic interpolation is used, neglecting departures from the hypothesis in Eq. (8) in the vicinity of the wall, one gets

$$\delta f_{i'}^{(2)}=2\alpha_i\mathbf{c}_i\cdot\mathbf{V}_0, \quad q<\tfrac{1}{2}, \tag{14}$$

$$\delta f_{i'}^{(2)} = \frac{2}{q(2q+1)} \alpha_i \mathbf{c}_i \cdot \mathbf{V}_0, \quad q \geqslant \frac{1}{2}. \tag{15}$$

With interpolation 0, one simply puts $q=1/2$ in the previous expressions.

Previous studies allow a good theoretical understanding of the "bounce-back" condition[19–21] or have given analytic solutions in particular cases.[25,26] We could make a detailed analysis of the Poiseuille flow that we shall discuss in sec. IV. First Eq. (2) will be linearized by removing nonlinear terms appearing in the expressions of the equilibrium values of the moments. Then we consider $N_L$ lattice nodes so that one time step of the system corresponds to a linear transformation from a vector $\mathbf{E}(t)$ to a vector $\mathbf{E}(t+1)$ in a $9N_L$ dimensional space. Standard linear algebra techniques can be used to determine the eigenvalues and eigenvectors of that transformation. One can then analyze the eigenvectors to select those that are most affected by the boundary. In practice $N_L$ is fairly large, say a few hundred except in particular cases, and the work has to be done numerically. We have obtained some partial results but cannot make general comments.

However we can make the following remarks. As indicated previously, the scheme includes linear variations of the macroscopic fluid velocity that one tries to simulate by LBE. It should possess at least first-order accuracy. In cases that have been analyzed in detail[20] simple "bounce-back" produces errors that are second order in mesh size. We therefore assume that our interpolation scheme will be no worse and have an accuracy consistent with that of LBE, which is second order.

The remainder of this paper deals with some applications of the proposed scheme showing no strong departure from the above-mentioned assumption.

## IV. TWO-DIMENSIONAL COUETTE AND POISEUILLE FLOWS

To test the proposed formulas, we first considered the two-dimensional (2-D) plane Couette flow with boundaries parallel to the $y$ axis. We have verified that the steady state flow for one fixed boundary (at $x=x_0$) and one boundary moving with velocity parallel to the axis $O_y$, $\mathbf{V}_0$ (at $x=x_1$) is given by

$$\mathbf{v}(x) = \frac{(x-x_0)}{(x_1-x_0)} \mathbf{V}_0 \tag{16}$$

for any value of $x_0$ and $x_1$ if we first determine the relevant values of $q$ for each vertical boundary. Note that the classic "bounce-back" conditions, say at nodes $x_0=1$ and $x_1=N_x$, lead to a channel located between 1/2 and $N_x+1/2$.

We then consider Poiseuille flow in a 2-D channel defined by two boundaries $y=\lambda x+\mu_1$ and $y=\lambda x+\mu_2$ on a mesh including $N_x \times N_y$ lattice points. The slope $\lambda$ is chosen such that particles leaving the channel on the right-hand side can be introduced on the left-hand side with a suitable shift in the $y$ coordinate ($\lambda$ is a rational number $i/j$ with $N_x$ a multiple of $j$). The flow is driven by applying a body force $F$ parallel to the solid boundaries. For a channel of width $w$, the macroscopic flow is parallel to the centerline of the channel with an amplitude of the fluid velocity given by

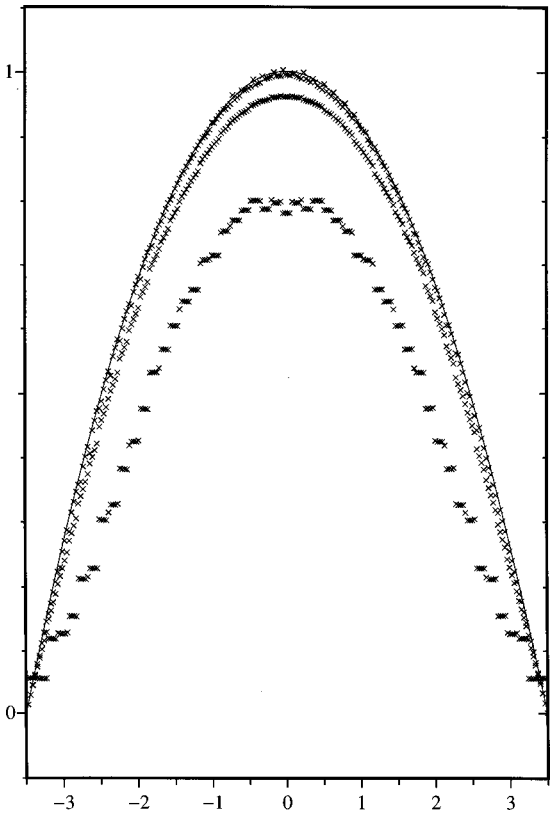


FIG. 2. Normalized value of the tangential velocity vs distance to the centerline for Poiseuille flow computed by LBE in a channel of width 7. Slope of boundaries 9/31. From bottom to top: interpolation 0, interpolation 1, interpolation 2. Solid line from Eq. (17).

$$V(z) = \frac{F}{2\nu}\left(z-\frac{w}{2}\right)\left(z+\frac{w}{2}\right), \tag{17}$$

where $z$ is the distance to the centerline of the channel $y=\lambda x+1/2(\mu_1+\mu_2)$ and $\nu$ the shear viscosity. As examples of the capabilities of LBE and boundary conditions to simulate such a situation, we show in Fig. 2 the values of the component of the LBE velocity parallel to the axis of the channel versus $z$ for all lattice points inside the channel. The prediction of Eq. (17) appears as the solid curve.

Going from interpolation 0 to 2 clearly improves the quality of the LBE simulation. An important point is that with interpolation 1 and better with interpolation 2, the LBE velocity goes to 0 on the boundary, whereas the interpolation 0 (as is well documented for boundaries parallel to $O_x$, $O_y$ or their bisector) leads to $V=0$ for $z=\pm(w/2+\delta)$ with $\delta$ depending on $w$ and the relaxation rates used for the LBE simulation.[20]

## V. FLOW INSIDE A TWO-DIMENSIONAL CIRCULAR CYLINDER

We consider the case of a LBE fluid inside a two-dimensional circular boundary of radius $R$ (centered at origin of the $xy$ plane). The initial conditions are (1) impulsively started circular flow, i.e., uniform density and flow at rest and

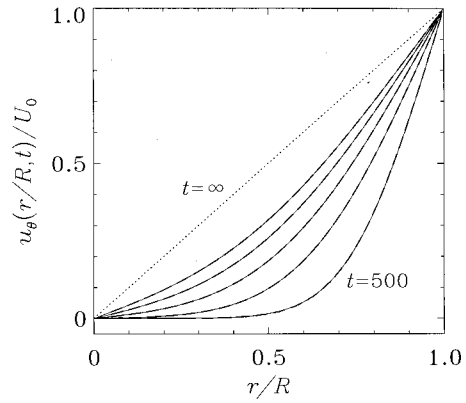


FIG. 3. 2-D flow in a rotating circular cylinder. Transient behavior of normalized tangential velocity $u_\theta/U_0$ as a function of normalized radius $r/R$ and time $t$. The solid and dashed lines are analytic and LBE simulation results, respectively, at $t=500$, 1000, 1500, 2000, and 2500. The dotted line is the asymptotic limit of the velocity at $t=\infty$. Note that $u_\theta(r,t=500)<u_\theta(r,t=1000)<u_\theta(r,t=1500)<u_\theta(r,t=2000)<u_\theta(r,t=2500)$.

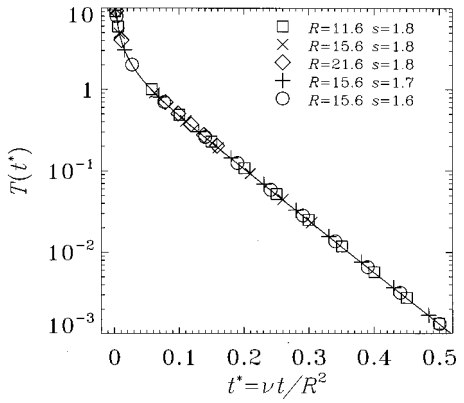


FIG. 4. Time-dependent amplitude of the torque (in units of $\nu U_\theta$) due to the momentum transfer between the fluid and the circular boundary vs reduced time, first index ($R$, radius of the circular boundary), second index ($s$ related to the shear viscosity) for the impulsively started circular boundary and the fluid at rest at $t=0$.

the cylinder impulsively starts with an angular velocity $\omega=U_\theta/R$, where $U_\theta$ is the tangential velocity of the cylinder, or (2) circular flow with the cylinder boundary at rest, taking as the initial state the steady state reached after a long time in situation (1).

For small values of $\omega$, the Navier–Stokes equations has a solution for the impulsively started circular flow:

$$u_\theta(r,t)=\frac{U_\theta r}{R}+w_\theta(r,t), \tag{18}$$

where

$$w_\theta(r,t)=\sum_k a_k J_1\left(\mu_k\frac{r}{R}\right)\exp\left(-\frac{\nu\mu_k^2}{R^2}t\right), \tag{19}$$

and $\nu$ is the kinematic shear viscosity, $\mu_k$ is the $k$th root of the Bessel function of order 1, [i.e., $J_1(\mu_k)=0$], and the coefficient $a_k$ comes from the initial conditions

$$a_k=\frac{2U_\theta}{\mu_k J_0(\mu_k)}. \tag{20}$$

Starting from rest $v_\theta(r,t)=\omega r+w_\theta(r,t)$, whereas the slowdown is just $-w_\theta(r,t)$.

The LBE simulations have been performed in the particular conditions indicated in the following. The radius of the circle is 15.2 lattice units, the relaxation rates (inverse of relaxation times appearing for instance in the BGK equations) have been chosen such that the shear viscosity is 0.018 52 (in nondimensional units).

Figure 3 compares the numerical results of $u_\theta(r,t)$ obtained by the LBE simulation to the analytic result of Eq. (18). There is no adjustable parameter in the LBE simulation in this case. The LBE results agree very well with the analytic solutions. It should be stressed that, in spite of the fact that the LBE algorithm uses Cartesian coordinates and is known to present anisotropies for excitations of short wavelengths,[23] the symmetry of the flow is well preserved in the present LBE simulation.

## VI. MOMENTUM TRANSFER ON THE BOUNDARY

The expressions for the unknown $f_i$ at boundary points $\mathbf{r}_l$ allow us to determine the momentum transfer. Let us consider again Fig. 1. We can consider that the final value of the population of particles with velocity to the left at $A$ corresponds to those coming from a fictitious state $B$. If $B$ was a fluid particle there would be a flux of momentum through a plane perpendicular to $AB$,

$$\phi=f_R^c+f_L(t+1). \tag{21}$$

As the wall is opaque to particles, $\phi$ is transferred to the wall. As the proposed scheme deals with directions of particle speeds one at a time there is a quantity $\phi_i$ for each direction $i$ and the total amount of momentum $\mathbf{P}_l$ transferred to the wall is obtained by summing $\phi_i\mathbf{c}_i$ over all $\mathbf{c}_i$ that cross the wall starting from fluid node $\mathbf{r}_l$.

For the Poiseuille flow of Sec. IV, we have verified that while reaching steady state, the change of the parallel component of the total linear momentum of the fluid during one time step is equal to the difference of the input of momentum $N_aF$ ($N_a$ being the number of "active" points where the force $F$ is applied) minus the transfer of momentum to the boundaries computed as indicated previously during the same time step.

To illustrate the use of the direct computation of the momentum transfer, we consider again the 2-D flow in a cylinder of Sec. V. Now we determine the torque applied to the fluid by the circle (either a driving or slowing torque depending on the situation). At each point $\mathbf{r}_l$ from which a particle gets affected by the boundary, we determine $\mathbf{r}_l\times\mathbf{P}_l$ and sum over all such points.

From the solution of Navier–Stokes equation [Eq. (19)], we can derive the theoretical value of this torque as

$$T(t)=2\pi R\nu\frac{dw_\theta(r,t)}{dr}, \tag{22}$$

where $v_\theta(r,t)$ is given by Eq. (19). We show in Fig. 4 the time dependence of torque (divided by $\nu U_\theta$) determined by the LBE simulation versus time (in units of $t_d=R^2/\nu$) for

several situations, together with the analytic solution for $T(t/t_d)/(\nu U_\theta)$. One can conclude that the LBE simulations lead to very satisfactory results whether the boundary is fixed or not.

Obviously the shape of the boundary can be chosen arbitrarily. In particular one can use the measurement of momentum transfer to determine lift and drag coefficients for wing sections. Work is in progress to estimate the accuracy of LBE predictions when the size of the sections is not very large.

## VII. FLOW PAST A 2-D PERIODIC ARRAY OF CYLINDERS

Flow through porous media has attracted much effort in the CFD community recently.[27,28] One simplified model for the flow is the flow past a periodic array of circular cylinders.[27,28] One may study just one cell of the array with periodic boundary conditions and a steady body force applied to the fluid to counteract the drag due to the cylinders. For small body forces, the steady state regime leads to a mean flow proportional to the force as was found by Darcy. This is usually expressed in the form

$$\mathbf{V} = -\frac{1}{\mu}\mathsf{K}\boldsymbol{\nabla} p, \tag{23}$$

where $\mathbf{V}$ is the mean seepage velocity, $\boldsymbol{\nabla} p$ the pressure gradient, $\mu$ the shear viscosity, and $\mathsf{K}$ the permeability tensor.

Theoretical results for $\mathsf{K}$ have been obtained with analytic expansions[27] or with accurate finite element CFD computations.[28] As we consider here a situation which is isotropic, $\mathsf{K}$ reduces to a scalar and we can consider the following quantity

$$Q \equiv K^{-1} = \frac{\text{mean force on the cylinder}}{\text{viscosity} \times \text{mean flux}} \tag{24}$$

to compare our data with the results of the studies mentioned previously, as a function of the fraction of the volume $C$ occupied by the cylinders. Note that this simplification does not apply at moderate Reynolds numbers.[29]

The finite element CFD computations used here are performed assuming periodic boundary conditions for the unit cell $\Omega_f$ (corresponding to the domain computed by LBE) and no-slip boundary conditions on the solid. The Stokes problem to be solved for the flow in the unit cell subject to an external pressure gradient $\boldsymbol{\lambda}$ with $|\boldsymbol{\lambda}| = 1$ (in terms of velocity $\mathbf{u}$ and pressure $p$) is

$$\begin{aligned} &-\nabla^2 \mathbf{u}(\boldsymbol{\lambda}) + \boldsymbol{\nabla} p(\boldsymbol{\lambda}) = \boldsymbol{\lambda}, \\ &\boldsymbol{\nabla} \cdot \mathbf{u}(\boldsymbol{\lambda}) = 0, \\ &\mathbf{u}(\boldsymbol{\lambda})|_{\Gamma_s} = 0, \\ &\mathbf{u}, p \quad \text{periodic.} \end{aligned} \tag{25}$$

The permeability tensor $\mathsf{K}$ is introduced to be

$$\mathsf{K} \cdot \boldsymbol{\lambda} = \frac{1}{\text{meas}(\Omega_f)} \int_{\Omega_f} \mathbf{u}(\boldsymbol{\lambda})\, dx\, dy. \tag{26}$$

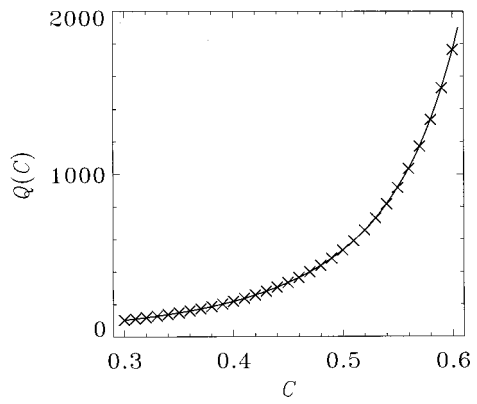


FIG. 5. Flow past a 2-D periodic array of cylinders. $Q$ (inverse of the permeability) computed by LBE method (solid line) and by finite element method ($\times$) as a function of concentration $C$.

The numerical solution is obtained by mixed finite element (P1/P2) based on an isoparametric nonuniform mesh. By denoting $\mathbf{u}$ and $p$ the velocity and pressure, the coupled system expressing the Stokes equations in weak form reads in matrix form:

$$\mathsf{A}\mathbf{u} + \mathsf{B}^t p = \mathbf{g}, \tag{27a}$$

$$\mathsf{B}u = 0. \tag{27b}$$

Eliminating the velocity, the so-called Uzawa approach yields an equation for the pressure which reads

$$\mathsf{A}\mathbf{u} = (\mathbf{g} - \mathsf{B}^t p) \Rightarrow \mathbf{u}, \tag{28a}$$

$$\mathsf{B}\mathsf{A}^{-1}\mathsf{B}^t p = \mathsf{B}\mathsf{A}^{-1}\mathbf{g} \Rightarrow p, \tag{28b}$$

where $\mathsf{B}\mathsf{A}^{-1}\mathsf{B}^t = \mathsf{U}$ is the Uzawa operator. An iterative algorithm based on the preconditioned GMRES method[30] is used to solve this system of coupled equations. This avoids the construction of the global $\mathsf{B}\mathsf{A}^{-1}\mathsf{B}^t$ operator. This step represents the projection of the velocity field into a divergence free subspace. This procedure has already been used for the sharp edged porous medium to compute in particular the permeability.[31]

For values of $C$ for which the results for $Q$ were given by Sangani and Acrivos,[27] the lattice Boltzmann results agree very well with the finite-element ones. These results are used to test the LBE technique.

We obtain a fairly good agreement with the Navier–Stokes results if we take the quadratic approximation for the unknown $f_i$ at boundaries as shown in Fig. 5. In addition we verify the isotropy of the LBE computation with very good accuracy when the center of the cylinder is located on one of the lattice nodes.

We have studied the convergence of the LBE results for some cases. As an example we show in Fig. 6 the relative difference $\|Q_{\text{LBE}}/Q_{\text{FE}} - 1\|$ for various values of the size $N_x$ of the domain in which the LBE computations are done, keeping the same value of $C$. We observe a tendency of the convergence as $1/N_x^2$, together with fluctuations. We compare in Fig. 6 the results obtained with the linear and the quadratic approximations. It is clear that the quadratic approximation leads to much improved data.

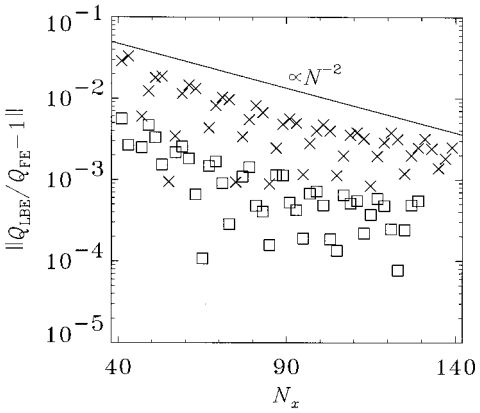


FIG. 6. Convergence of the factor $Q$ computed by LBE with quadratic ($\square$) and linear interpolation ($\times$) vs computational domain size.

To test in more detail the present LBE technique, we look at the effect of choosing the center of the cylinder to be at a point $(l_x+q,l_y)$ for integers $l_x$ and $l_y$, and $0\leqslant q\leqslant 1$. We show in Fig. 7 the variation $(Q_x/Q_{\mathrm{FE}}-1)$ and $(Q_y/Q_{\mathrm{FE}}-1)$ for the linear and quadratic interpolation formulas. We can observe some anisotropy and the fact that fluctuations are smaller with the quadratic interpolation. These results are shown for a domain size of $N_x\times N_y=53^2$ and $C=0.5$, leading to a minimum width of the channels between neighboring cylinders of 10.7 lattice spacing.

Similar to Sec. VI, we can compare the momentum transfer computed on the boundary with the amount of momentum used to drive the fluid by applying some kind of body force (gravity). It is found that when steady state is reached the two quantities agree with high accuracy. This can be interpreted as the result of a correct implementation of the conservation of linear momentum in the various steps of the LBE algorithm (collisions, advection, and interactions with the boundary).

## VIII. CONCLUSION

A simple and efficient way to implement moving and curved boundaries in LBE simulations has been described. Tests on nontrivial cases allow one to get confidence and therefore to contribute to support the LBE technique as a useful technique for computational fluid dynamics. The computational cost is typically a few percent of the LBE simulation even when the present technique is applied to the three-dimensional nineteen-velocity model. The initial generation of the lists of boundary points and of the corresponding values for the coefficients $q$ is orders of magnitude faster than the grid generation required by finite-element computations.

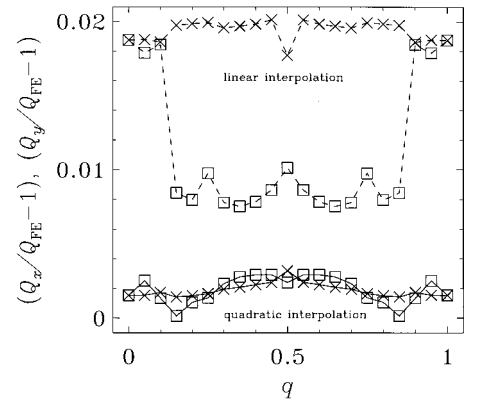


FIG. 7. Dependence of the factor $Q$ computed by LBE vs displacement of the center of the cylinder along $Ox$. Dashed curves and solid lines correspond, respectively, to linear and quadratic interpolation. $\times$ and $\square$ correspond, respectively, to the force being applied along $x$ and $y$ directions.

## ACKNOWLEDGMENTS

The authors wish to thank Dr. D. d'Humières and Dr. L. S. Luo for very useful discussions.

[1] U. Frisch, B. Hasslacher, and Y. Pomeau, "Lattice gas automata for the Navier–Stokes equation," Phys. Rev. Lett. **56**, 1505 (1986).
[2] U. Frisch, D. d'Humières, B. Hasslacher, P. Lallemand, Y. Pomeau, and J.-P. Rivet, "Lattice gas hydrodynamics in two and three dimensions," Complex Syst. **1**, 649 (1987).
[3] G. McNamara and G. Zanetti, "Use of the Boltzmann equation to simulate lattice gas automata," Phys. Rev. Lett. **61**, 2332 (1988).
[4] F. J. Higuera and J. Jiménez, "Boltzmann approach to lattice gas simulations," Europhys. Lett. **9**, 663 (1989).
[5] F. J. Higuera, S. Succi, and R. Benzi, "Lattice gas dynamics with enhanced collisions," Europhys. Lett. **9**, 345 (1989).
[6] H. Chen, S. Chen, and W. H. Matthaeus, "Recovery of the Navier–Stokes equations using a lattice gas Boltzmann method," Phys. Rev. A **45**, R5339 (1992).
[7] Y. H. Qian, D. d'Humières, and P. Lallemand, "Lattice BGK models for Navier–Stokes equation," Europhys. Lett. **17**, 479 (1992).
[8] R. Benzi, S. Succi, and M. Vergassola, "The lattice Boltzmann equation: Theory and applications," Phys. Rep. **222**, 145 (1992).
[9] S. Chen and G. D. Doolen, "Lattice Boltzmann method for fluid flows," Annu. Rev. Fluid Mech. **30**, 329 (1998).
[10] X. He and L.-S. Luo, "Lattice Boltzmann model for the incompressible Navier–Stokes equation," J. Stat. Phys. **88**, 927 (1997).
[11] D. d'Humières, "Generalized lattice-Boltzmann equations," in *Rarefied Gas Dynamics: Theory and Simulations*, Progress in Astronautics and Aeronautics Vol. 159, edited by B. D. Shizgal and D. P. Weaver (AIAA, Washington, DC, 1992).
[12] D. P. Zeigler, "Boundary conditions for the lattice Boltzmann simulations," J. Stat. Phys. **71**, 1171 (1993).
[13] O. Behrend, "Solid boundaries in particle suspension simulations via lattice Boltzmann method," Phys. Rev. E **52**, 1164 (1995).
[14] P. A. Skordos, "Initial and boundary conditions for the lattice Boltzmann method," Phys. Rev. E **48**, 4823 (1993).
[15] D. R. Noble, S. Chen, J. G. Georgiadis, and R. O. Buckius, "A consistent hydrodynamic boundary condition for the lattice Boltzmann method," Phys. Fluids **7**, 203 (1995).
[16] T. Inamuro, M. Yoshino, and F. Ogino, "A nonslip boundary condition for the lattice Boltzmann simulations," Phys. Fluids **7**, 2928 (1995).
[17] S. Chen, D. Martinez, and R. Mei, "On boundary conditions in lattice Boltzmann method," Phys. Fluids **8**, 2527 (1996).
[18] R. Mei, L.-S. Luo, and W. Shyy, "An accurate curved boundary treatment in lattice Boltzmann method," J. Comput. Phys. **155**, 307 (1999).
[19] R. Cornubert, D. d'Humières, and D. Levermore, "A Knudsen layer theory," Physica D **47**, 241 (1991).
[20] I. Ginzburg and P. Adler, "Boundary flow condition analysis for the three-dimensional lattice Boltzmann method," J. Phys. II **4**, 191 (1994).
[21] I. Ginzburg and D. d'Humières, "Local second-order boundary methods for lattice Boltzmann models," J. Stat. Phys. **84**, 927 (1996).
[22] I. V. Karlin, S. Succi, and S. Orszag, "Lattice Boltzmann method for irregular grids," Phys. Rev. Lett. **82**, 5245 (1999).
[23] P. Lallemand and L.-S. Luo, "Theory of the lattice Boltzmann method: Dispersion, dissipation, isotropy, Galilean invariance and stability," Phys. Rev. E **61**, 6546 (2000).
[24] O. Filippova and D. Hänel, "Grid refinement for lattice BGK models," J. Comput. Phys. **147**, 219 (1998).

[25]X. He, Q. Zou, L.-S. Luo, and M. Dembo, ''Analytic solutions of simple flows and analysis of non slip boundary conditions for the lattice Boltzmann BGK model,'' J. Stat. Phys. **87**, 115 (1997).
[26]L.-S. Luo, ''Analytic solutions of linearized lattice Boltzmann equation for simple flows,'' J. Stat. Phys. **88**, 913 (1997).
[27]A. S. Sangani and A. Acrivos, ''Slow flow past periodic arrays of cylinders with applications to heat transfer,'' Int. J. Multiphase Flow **8**, 193 (1982). *Note that the coefficient of $b_n$ at the end of their Eq. (11) should be* $+(2n-1)$.
[28]M. Firdaouss, J. L. Guermond, and P. Le Quéré, ''Non linear corrections to Darcy's law at low Reynolds numbers,'' J. Fluid Mech. **343**, 331 (1997).
[29]D. L. Koch and A. J. Ladd, ''Moderate Reynolds number flows through periodic and random arrays of aligned cylinders,'' J. Fluid Mech. **349**, 31 (1997).
[30]Y. Saad and M. H. Schultz, ''GMRES: A generalized minimal residual algorithm for solving nonsymmetric linear systems,'' SIAM J. Sci. Comp. **7**, 856 (1986).
[31]M. Firdaouss, J. L. Guermond, and D. Lafarge, ''Some remarks on the acoustic parameters of sharp-edged porous media,'' Int. J. Eng. Sci. **36**, 1035 (1998).